p47*phox* is required for atherosclerotic lesion progression in *ApoE*$^{-/-}$ mice

See related Commentary on pages 1423–1424.

Patricia A. Barry-Lane,[1] Cam Patterson,[2,3] Marié van der Merwe,[2] Zhaoyong Hu,[1] Stephen M. Holland,[4] Edward T.H. Yeh,[5] and Marschall S. Runge[2]

[1]Sealy Center for Molecular Cardiology, University of Texas Medical Branch, Galveston, Texas, USA
[2]University of North Carolina at Chapel Hill, Carolina Cardiovascular Biology Center, Division of Cardiology and Department of Medicine, and
[3]Lineberger Comprehensive Cancer Center, Chapel Hill, North Carolina, USA
[4]Laboratory of Host Defenses, National Institute of Allergy and Infectious Diseases, Bethesda, Maryland, USA
[5]Research Center for Cardiovascular Diseases, University of Texas–Houston Health Science Center, Houston, Texas, USA

Address correspondence to: Marschall S. Runge, Department of Medicine, University of North Carolina at Chapel Hill, 3033 Old Clinic Building, Campus Box 7005, Chapel Hill, North Carolina, 27599-7005, USA.
Phone: (919) 966-4468; Fax: (919) 966-5775; E-mail: mrunge@med.unc.edu.

Received for publication December 5, 2000, and accepted in revised form September 24, 2001.

NADPH oxidase is upregulated in smooth muscle cells (SMCs) in response to growth factor stimulation, concomitant with increased reactive oxygen species (ROS) production. We investigated the role of ROS production by NADPH oxidase in SMC responses to growth factors and in atherosclerotic lesion formation in *ApoE*$^{-/-}$ mice. SMCs from wild-type, p47*phox*$^{-/-}$, and gp91*phox*$^{-/-}$ mice differed markedly with respect to growth factor responsiveness and ROS generation. p47*phox*$^{-/-}$ SMCs had diminished superoxide production and a decreased proliferative response to growth factors compared with wild-type cells, whereas the response of gp91*phox*$^{-/-}$ SMCs was indistinguishable from that of wild-type SMCs. The relevance of these in vitro observations was tested by measuring atherosclerotic lesion formation in genetically modified (wild-type, p47*phox*$^{-/-}$, ApoE$^{-/-}$, and ApoE$^{-/-}$/p47*phox*$^{-/-}$) mice. *ApoE*$^{-/-}$/p47*phox*$^{-/-}$ mice had less total lesion area than *ApoE*$^{-/-}$ mice, regardless of whether mice were fed standard chow or a high-fat diet. Together, these studies provide convincing support for the hypothesis that superoxide generation in general, and NADPH oxidase in particular, have a requisite role in atherosclerotic lesion formation, and they provide a rationale for further studies to dissect the contributions of ROS to vascular lesion formation.

J. Clin. Invest. **108**:1513–1522 (2001). DOI:10.1172/JCI200111927.

Introduction

Oxidative stress is hypothesized to be an important contributor to the pathophysiology of vascular diseases such as atherosclerosis, hypertension, and diabetic microvascular disease (1–4). Reactive oxygen species (ROS) have been implicated in many aspects of vascular injury and lesion development, including lipoprotein oxidation, foam cell formation, smooth muscle cell (SMC) hypertrophy, and endothelial cell damage (5, 6). Although ROS generation was originally thought to be limited to phagocytic cells, which contain the prototypical NADPH oxidase, it is now well accepted that nonphagocytic cell types, such as fibroblasts, glomerular cells, and osteoclasts, also express components of NADPH oxidase and generate ROS (7–11). Of particular relevance with respect to vascular disease, endothelial cells, macrophages, and vascular SMCs — all components of atherosclerotic lesions — are also sources of ROS (12–14).

The NADPH oxidase found in phagocytic cells is a multisubunit complex consisting of cytosolic and membrane-bound components (15). The membrane-bound subunits include gp91*phox* and p22*phox*, and comprise the catalytic, flavin-containing portion of the oxidase. The p47*phox* subunit is a cytosolic component; one of the early steps in oxidase activation is phosphorylation and translocation of p47*phox* to the membrane (16). Although NADPH oxidase is less well characterized in nonphagocytic cells, physiologically relevant generation of ROS and expression of NADPH oxidase subunits are present in vascular tissue. The vascular endothelium expresses p22*phox*, p47*phox*, and gp91*phox* (17, 18). Cultured SMCs express both p22*phox* and p47*phox* (19, 20), and expression of p22*phox*, p47*phox*, p67*phox*, and gp91*phox* has been demonstrated in the vascular adventitia (21). Relevant to the present study, characterization of the NADPH oxidase in SMCs has indicated that, in these cells, the function of the catalytic gp91*phox* subunit is probably replaced by a homologue (a member of the *nox* family) that has functional and structural similarity to gp91*phox* (22, 23).

In addition to differences in expression of oxidase components, the phagocytic-cell and SMC oxidases differ with regard to substrate preference and enzyme activity. The phagocytic-cell oxidase utilizes NADPH preferentially, whereas SMC and other nonphagocytic-cell oxidases can also use NADH for ROS generation.

Nonphagocytic cells also produce less superoxide (O_2^-) after oxidase activation than phagocytic cells do (24). The low level of ROS generated by the nonphagocytic-cell enzyme is more apt to alter the redox potential of the cell and mediate cell signals than to act as a host defense. Together, these data indicate that the SMC NADPH oxidases differ from their counterparts in phagocytic cells, and that the differences in components correlate with differences in the cellular functions of these oxidases.

ROS production by the cytosolic NADPH oxidase complex is a critical signal regulating vascular responses to stimulation. Treatment of SMCs with PDGF or thrombin induces O_2^- and hydrogen peroxide (H_2O_2) production, and inhibition of ROS production blocks SMC proliferation (25, 26). In addition, angiotensin II–induced SMC hypertrophy is dependent on ROS production (4, 19). Thrombin-stimulated O_2^- production in SMCs increases NADH consumption, which is inhibited by the flavin-containing enzyme inhibitor diphenyliodonium (25). Coincident with ROS generation, p47*phox* expression and phosphorylation are increased in SMCs after thrombin stimulation. These data support the hypothesis that NADPH oxidase is involved in growth factor–induced SMC proliferation and suggest that this oxidase system plays an important role in atherogenesis.

The experiments described were designed to characterize the role of the p47*phox* subunit of NADPH oxidase in SMC growth in cultured cells, and to determine whether deficiency in NADPH oxidase activity alters atherosclerotic lesion formation in the ApoE$^{-/-}$ murine model for atherosclerosis. SMCs from mice genetically deficient in NADPH oxidase (p47*phox*$^{-/-}$ and gp91*phox*$^{-/-}$ mice) were used to resolve the importance of these two subunits in vascular cell signaling. SMCs lacking p47*phox* have attenuated responsiveness to growth factors in terms of both ROS generation and growth when compared with wild-type SMCs. Mice deficient in both ApoE and p47*phox* were generated to determine the importance of NADPH oxidase in atherosclerotic lesion formation. Analysis of oil red O–positive lesions in the aortic tree showed that ApoE$^{-/-}$/p47*phox*$^{-/-}$ mice had decreased lesion area compared with ApoE$^{-/-}$ mice, even though lesions in the aortic sinus showed no differences, consistent with previous findings (27, 28).

Methods

Animals and diet. Wild-type C57BL/6J mice, mice deficient in gp91*phox*, and ApoE-deficient mice were obtained from The Jackson Laboratory (Bar Harbor, Maine, USA). The gp91*phox*-deficient and ApoE-deficient mice were both on C57BL/6J backgrounds. p47*phox*-deficient mice were backcrossed four times to C57BL/6J mice. ApoE$^{-/-}$ mice were bred to p47*phox*$^{-/-}$ mice to create mice deficient in both proteins (ApoE$^{-/-}$/p47*phox*$^{-/-}$ mice). Age-matched, sibling male mice of both ApoE$^{-/-}$ and ApoE$^{-/-}$/p47*phox*$^{-/-}$ genotypes were used. Genotypes were determined by PCR amplification of tail DNA. Because of concerns that some p47*phox*$^{-/-}$ mice had been contaminated with a deletion at the IFN-γ locus, all mice were genotyped at this locus and were found to be wild-type. Animals were maintained in a 22°C room with a 12-hour light/dark cycle and given free access to food and water. Mice on a normal chow diet were maintained on pellet rodent chow (Harlan Teklad, Madison, Wisconsin, USA) until 30 weeks of age. Mice on the high-fat diet were maintained on rodent chow until 8 weeks of age, then fed a high-fat, atherogenic diet (15% fat by weight, Harlan Teklad), for 10 weeks. Blood was collected by cardiac puncture in tubes containing EDTA, and the plasma was stored at –20°C until analysis.

Cell culture. SMCs were isolated from aortas of wild-type, p47*phox*$^{-/-}$, and gp91*phox*$^{-/-}$ animals. The aortas were carefully dissected to remove excess connective tissue, then minced and digested in collagenase, elastase, and soybean trypsin inhibitor (29) at 37°C for 1 hour. The cells were plated in DMEM containing 10% FCS. Cells were determined to be SMCs by morphology and expression of smooth muscle α-actin. RT-PCR and Western blotting were performed to confirm the absence of p47*phox* and gp91*phox* mRNA and protein in cells derived from p47*phox*$^{-/-}$ and gp91*phox*$^{-/-}$ mice.

^{3}H-thymidine incorporation. SMCs grown to near confluence in six-well plates were made quiescent by serum starvation. Cells were treated with bovine serum (10%) or thrombin (2 U/ml) or maintained in serum-free medium for an additional 24 hours and labeled with methyl-^{3}H-thymidine at 1 μCi/ml during the last 3 hours of this time period. After labeling, the cells were washed with PBS and fixed in cold 10% trichloroacetic acid, and then washed with 95% ethanol. Incorporated ^{3}H-thymidine was extracted in 0.2 M NaOH and measured in a liquid scintillation counter (30). Values were expressed as the mean ± SD from six wells, and are representative of three separate experiments.

Western blot analysis. Growth-arrested SMCs were treated with the designated growth factors, and cell lysates were prepared. Immunoblotting was performed as described previously (31). Antibodies used were polyclonal anti-human p47*phox* (a kind gift of Bernard Babior, The Scripps Research Institute, La Jolla, California, USA) and peroxidase-labeled goat anti-rabbit IgG (Roche Molecular Biochemicals, Indianapolis, Indiana, USA). Mouse spleen lysate was a positive control for p47*phox* expression. Membrane fractions from SMCs were separated as described (32). Cells were lysed in a buffer containing 100 mM Tris-HCl, pH 7.4, and 2% Triton X-100, and the cytoskeleton was pelleted by centrifugation at 15,000 *g* for 5 minutes. The supernatant from this centrifugation was centrifuged at 100,000 *g* for 2.5 hours. The supernatant from this centrifugation was considered the cytosol, and the insoluble pellet was considered the membrane fraction. Immunoblot analysis was performed on fractions from equivalent numbers of cells. Densitometric

analyses were performed on at least three individual experiments, and results are expressed in arbitrary units as the mean ± SD.

RT-PCR for p47phox. SMCs were growth-arrested in 100-mm culture dishes and treated with or without thrombin (2 U/ml). Total RNA was isolated by cesium chloride ultracentrifugation. cDNA was obtained by transcription of RNA (2 μg) with Moloney murine leukemia virus reverse transcriptase, and PCR amplification was performed with Taq polymerase (Stratagene Inc., La Jolla, California, USA). For the PCR, a set of primers generated from the mouse neutrophil p47*phox* sequence (33) was used to amplify a 615-bp fragment of the p47*phox* gene product (P47-1, 5′-ACATCACAGGCCCCATCATCCTTC-3′; and P47-2, 5′-ATGGATTGTCCTTTGTGCC-3′). This fragment contains sequences coding for amino acids 160–361 of the mouse neutrophil p47*phox* protein (33). Simultaneous amplification was performed with primers specific to the β-actin gene, generating an 838-bp product, as an internal control. A cycle number of 30 was chosen for the PCR, based on preliminary experiments, to ensure that amplification remained within the linear range. Band intensities were determined by densitometry. Experiments were repeated three times, and the results were expressed as the mean ± SD.

Aconitase and fumarase activity. Aconitase is a citric acid cycle enzyme that is inactivated by O_2^- and has been used as a measure of ROS generation in cultured cells (34). Cells were plated in 100-mm dishes, made quiescent, and treated with growth factors for 1 hour. The cells were rinsed with ice-cold PBS and scraped into 15-ml conical tubes in 5 ml of homogenization buffer consisting of 50 mM Tris-HCl (pH 7.6), 1 mM cysteine, 1 mM citrate, and 0.6 mM $MnCl_2$. Cells were pelleted and transferred to 500 μl of cold homogenization buffer. The pellet was dispersed by vortexing, and lysed by sonication. Lysate (50 μl) was added to 200 μl of assay buffer (50 mM Tris-HCl (pH7.6), 30 mM citrate, 0.6 mM $MnCl_2$, 0.2 mM $NADP^+$, and 2 U/ml isocitrate dehydrogenase) in 96-well plates, in triplicate. Production of NADPH was determined by reading absorbance at 340 nm every 60 seconds for 60 minutes. Results are averages of triplicates ± SD and are representative of three separate experiments. Aconitase activity was normalized for protein per sample. The specificity of this assay was confirmed by pretreating cells with polyethylene glycol–conjugated superoxide dismutase (10 U/ml) 30 minutes prior to growth factor stimulation. Fumarase activity in cell lysates was measured by monitoring the increase in absorbance at 240 nm at 25°C in a 0.1-ml reaction mixture containing 30 mM potassium phosphate (pH 7.4), 0.1 mM EDTA, and 5 mM L-malate.

Immunohistochemistry. Immunostaining for p47*phox* and α-actin was performed on mouse aorta sections fixed in 4% paraformaldehyde. Slides were incubated with 0.3% H_2O_2 for 30 minutes and blocked with normal goat serum in PBS containing 0.1% BSA and 0.1% Tween 20 for 30 minutes. A 1:100 dilution of antibody (or normal rabbit IgG as a control) was applied to the slides and they were left for 12 hours at 4°C. Slides were then washed, incubated with goat anti-rabbit secondary antibody, and processed using the ABC Staining Kit (Vector Laboratories Inc., Burlingame, California, USA). p47*phox* staining was visualized with peroxidase using diaminobenzidine as a chromogen to yield a brown reaction product. For colocalization experiments, sections were stained with a monoclonal mouse anti–smooth muscle α-actin antibody (Novocastra Laboratories Inc., Burlingame, California, USA), which was detected with a horse anti-mouse IgG, and visualized with peroxidase using diaminobenzidine as a chromogen to yield a brown reaction product. The sections were also stained with the anti-p47*phox* antibody as above, and visualized with Vector Blue (Vector Laboratories Inc.) as a substrate. After counterstaining with hematoxylin, slides were dehydrated and permanently mounted.

Quantification of atherosclerotic lesions. Atherosclerosis in the aortas of the various murine models studied was measured by quantitation of oil red O–positive lesions that were morphologically consistent with atherosclerosis. This analysis was performed for lesions both within the aortic sinus and throughout the aorta, as described (35, 36). Areas of aortic sinus lesions were determined by serial sections of fresh-frozen hearts embedded in OCT medium (Sakura Finetek, Torrance, California, USA). Sections (10 μm thick) were taken throughout the aortic sinus (400 μm). Every other section was stained with oil red O and counterstained with hematoxylin. Lesion area of the whole aortic tree was also determined. Aortas were dissected from the heart to the bifurcation (taken from the same mice that were used for aortic sinus analysis). The vessels were rinsed in PBS and dissected to remove connective tissue and attached fat. The vessels were opened longitudinally and fixed overnight in 3.7% formaldehyde. Tissues were rinsed in PBS and stained with oil red O. Whole mounts of the vessels were prepared, photographed, and digitized. Oil red O–positive lesions were delineated and analyzed using NIH Image software (NIH, Bethesda, Maryland, USA). Values are presented as mean ± SD (n = 12 for each group).

Dihydroethidium labeling of aortas. To measure ROS production in vessels in situ, frozen cross sections of aortas were stained with dihydroethidium (DHE) using a previously validated method (37, 38). In the presence of O_2^-, DHE is converted to the fluorescent molecule ethidium, which can then label nuclei by intercalating with DNA. Fresh-frozen cross sections of aorta isolated from wild-type and p47*phox*$^{-/-}$ animals (10 μm) were stained with 10 μM DHE (Molecular Probes Inc., Eugene, Oregon, USA) for 5 minutes, rinsed, mounted, and observed using fluorescent microscopy. Results were pixilated and quantified using NIH Image software, and expressed as the mean ± SD of four aortas from each strain of mouse.

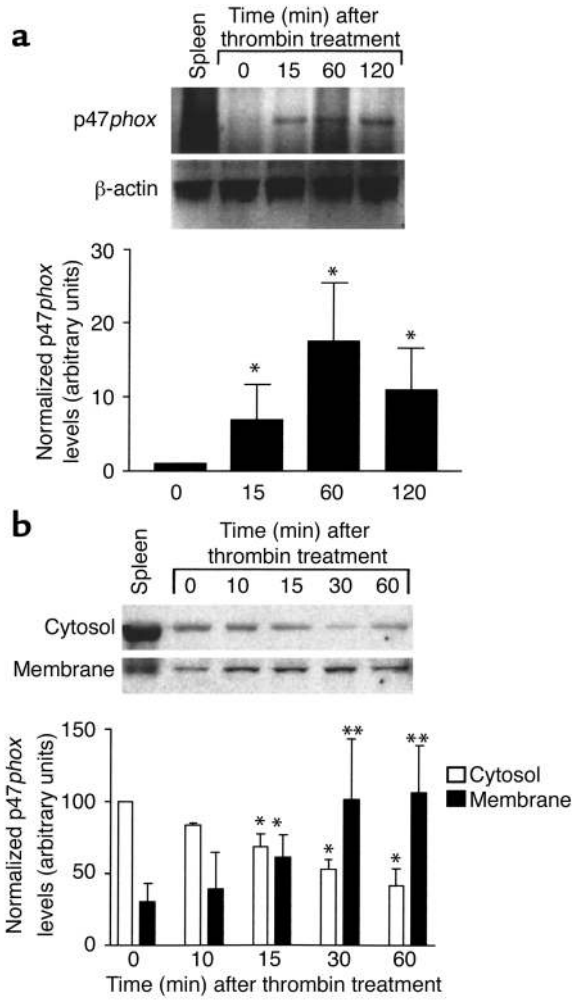

Figure 1
(**a**) RT-PCR of p47*phox* and β-actin in wild-type SMCs after thrombin stimulation (2 U/ml). There is induction of p47*phox* mRNA by 15 minutes after treatment. The first lane is control RNA from mouse spleen lysate. Results were quantified by densitometry and expressed as the mean ± SD of three experiments. **P* < 0.05 compared with untreated SMCs. (**b**) Western blot analysis of p47*phox* protein from membrane and cytosolic fractions of SMCs following thrombin stimulation. Results were quantified by densitometry and expressed as the mean ± SD from three experiments. **P* < 0.05 compared with untreated cytoplasmic fractions. ***P* < 0.05 compared with untreated membrane fractions.

Macrophage homing. Macrophages were recruited from wild-type and p47*phox*$^{-/-}$ mice by intraperitoneal injection of thioglycolate. Macrophages were isolated by attachment to Petri dishes and labeled with fluorescent microbeads. The labeled macrophages were counted, and 5×10^5 of them were injected into ApoE$^{-/-}$ mice via the tail vein. Forty-eight hours later, tissues were harvested from the ApoE$^{-/-}$ animals, embedded in OCT, and snap frozen in liquid nitrogen. Sections were made through the aorta, and the number of macrophages attached to or embedded in lesions was determined for each animal. The liver from each mouse was also dissected and frozen for sectioning to confirm loading of macrophages into the recipient mouse.

Results

p47phox RNA and protein are present in mouse SMCs and are regulated by thrombin. We previously reported that inhibition of NADPH oxidase in human SMCs inhibits thrombin-induced growth signaling (25). To determine whether a similar NADPH oxidase system was active in mouse SMCs, we examined whether p47*phox* mRNA and protein were expressed in wild-type mouse SMCs. Mouse p47*phox* mRNA was detected by RT-PCR in SMCs (Figure 1a). The basal level of p47*phox* mRNA increased within 15 minutes of thrombin stimulation (2 U/ml). This increase reached a maximum 15-fold induction and was sustained for at least 2 hours after addition of thrombin. We measured p47*phox* protein expression in cellular fractions isolated from SMCs treated with thrombin by Western blot analysis (Figure 1b). Because a critical step in activation of the NADPH oxidase protein complex involves phosphorylation and translocation of p47*phox* from the cytosol to the membrane fraction, we investigated whether thrombin induced p47*phox* translocation in these SMCs. Membrane and cytosolic fractions were isolated from wild-type SMCs treated with thrombin. Within 15 minutes of treatment, p47*phox* protein was significantly increased in the membrane fraction. Enrichment of p47*phox* in the membrane fraction was maximal at 30 minutes and was coincident with depletion of p47*phox* from the cytosol.

Expression of p47phox is necessary for SMC proliferation in response to thrombin and serum. SMCs isolated from wild-type, p47*phox*$^{-/-}$, and gp91*phox*$^{-/-}$ animals were examined in culture to determine whether these NADPH oxidase subunits are necessary for SMCs to respond to growth factors. Aortic SMCs were isolated and amplified in culture. After reaching quiescence, the cells were treated overnight with either thrombin (2 U/ml) or FBS (10%). The growth response of the cells was determined by incorporation of ^{3}H-thymidine as a marker for DNA replication (Figure 2a). Wild-type SMCs had an approximately threefold greater incorporation of ^{3}H-thymidine in response to both serum and thrombin stimulation than did p47*phox*$^{-/-}$ SMCs. Interestingly, there was no difference in growth responses between wild-type and gp91*phox*$^{-/-}$ cells after either serum or thrombin stimulation, consistent with previous observations that there is a gp91*phox* homologue present in SMCs (18). Results of thymidine uptake were confirmed by cell-count experiments, which demonstrated that the number of p47*phox*$^{-/-}$ SMCs was 31% that of wild-type SMCs after 9 days in culture (Figure 2b).

Growth factor–stimulated ROS production is impaired in p47phox$^{-/-}$ but not gp91phox$^{-/-}$ cells. Having demonstrated differences in ^{3}H-thymidine incorporation in cells lacking p47*phox*, we next investigated whether this correlated with a decrease in O_2^- production. O_2^- production was determined in cells indirectly by measuring aconitase activity after growth factor treatment (Figure 3a). p47*phox*-deficient cells had lower basal levels of O_2^- production (higher aconitase activity) than did wild-type and gp91*phox*-deficient cells, and also had attenuated

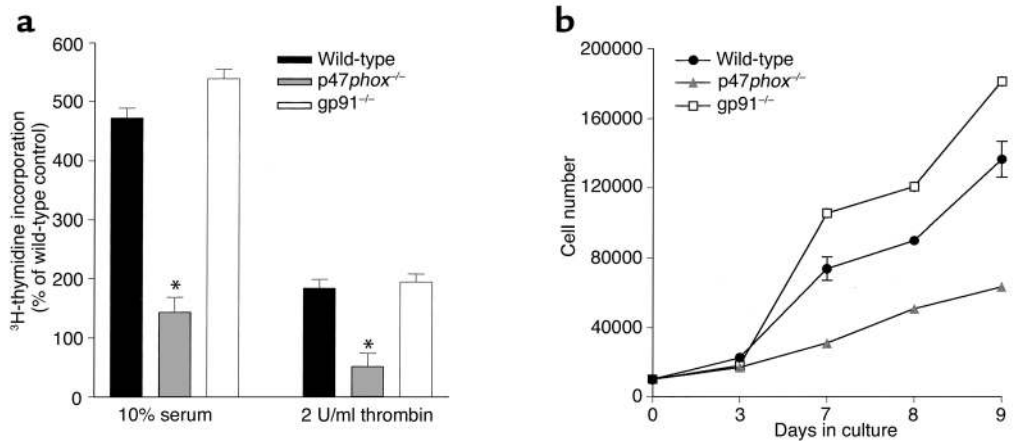

Figure 2
Proliferative capacity is decreased in p47*phox*$^{-/-}$ SMCs compared with wild-type SMCs after growth factor stimulation. (**a**) Wild-type, p47*phox*-, or gp91*phox*-deficient SMCs were treated with the indicated concentrations of thrombin or serum, and uptake experiments were performed using thymidine as a marker for DNA synthesis. Results are shown as the mean of six wells ± SD, and are representative of three separate experiments. *$P < 0.05$ compared with wild-type SMCs. (**b**) Growth curve analysis of wild-type, p47*phox*-, or gp91*phox*-deficient SMCs plated at equivalent densities and allowed to proliferate for the indicated time periods. Results are shown as the mean of three wells ± SD and are representative of three separate experiments.

growth factor–responsive O_2^- production. The reduction in aconitase activity was inhibited by pretreatment of cells with superoxide dismutase. The specificity of these experiments was determined by measuring fumarase activity, which represents another step in the citric acid cycle and is insensitive to O_2^--induced inactivation. No differences were found between cell types in either basal or inducible fumarase activity (Figure 3b). Taken together with our proliferation experiments, these results support the theory that O_2^- produced by NADPH oxidase is necessary for normal SMC response to growth factors, and that the p47*phox* subunit of NADPH oxidase is necessary for SMC response to growth factor stimulation, whereas the gp91*phox* protein is not. Consistent with these observations, we also found that conversion of DHE to ethidium, a sensitive marker for O_2^- generation, was markedly attenuated in p47*phox*-deficient cells (see Supplemental Data 1, www.jci.org/cgi/content/full/108/10/1513/DC1).

Expression of p47phox in aortas of atherosclerotic mice. We performed immunohistochemical analyses to determine whether p47*phox* was also expressed in vascular cells in vivo. Using a specific anti-p47*phox* antibody (see Supplemental Data 2, www.jci.org/cgi/content/full/108/10/1513/DC2), we found that p47*phox* expression is expressed in cells within aortic lesions in ApoE$^{-/-}$ mice (Figure 4, c and d) and in normal aorta (Figure 4a). Adventitial, and to a lesser extent endothelial, staining is present in all specimens, and luminal endothelial cell expression is most prominent in diseased arteries. Staining of mural cells is essentially absent in nondiseased aortic specimens (Figure 4a), but is prominent in diseased aortas (Figure 4, b–d). Some of these cells have large nuclei, are within fibrous plaques, and do not colocalize with α-actin (yellow arrows), but do colocalize with macrophage markers (not shown). Others within the plaque shoulder and in

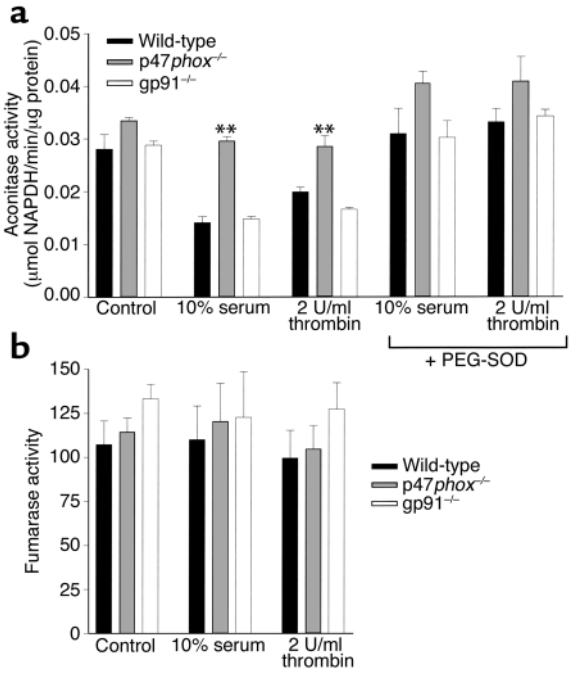

Figure 3
Intracellular ROS production is decreased in p47*phox*$^{-/-}$ SMCs compared with wild-type SMCs. (**a**) p47*phox*-deficient SMCs have significantly less O_2^- production, as reflected by attenuation of the decrease in aconitase activity, following thrombin and serum stimulation (**$P < 0.05$) than do wild-type SMCs. There is no difference in O_2^- production between wild-type and gp91*phox*-deficient cells. The reduction in aconitase activity is reversed by pretreatment with polyethylene glycol–conjugated superoxide dismutase (PEG-SOD). (**b**) Fumarase activity was similar in wild-type, p47*phox*$^{-/-}$, and gp91*phox*$^{-/-}$ SMCs, demonstrating the specificity of the aconitase assays described in **a**.

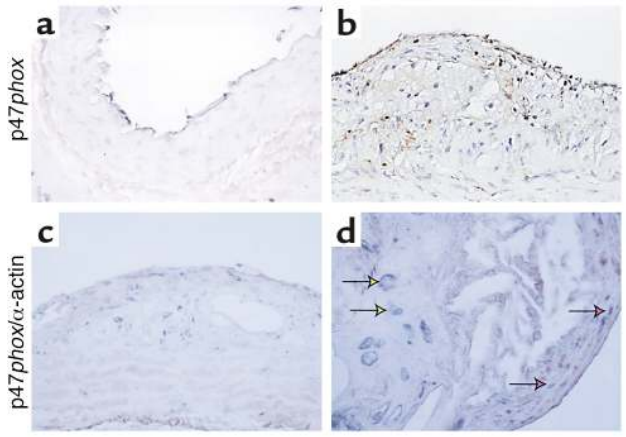

Figure 4
Expression of p47*phox* in wild-type and ApoE$^{-/-}$ atherosclerotic arteries. Representative arterial sections from wild-type (**a**) and ApoE$^{-/-}$ (**b**–**d**) mice. Sections were stained for antibodies against p47*phox* alone (**a** and **b**, brown chromogen), or simultaneously with antibodies against p47*phox* (blue) and α-actin (brown). Yellow arrows indicate cells in the plaque staining positive for p47*phox* alone, and red arrows indicate neointimal cells staining positive for both p47*phox* and α-actin.

the neointima overlying the plaque are α-actin–positive and therefore are presumptively SMCs (red arrows). This upregulation of p47*phox* expression in SMCs in situ is consistent with our demonstration of increased p47*phox* expression after balloon injury in rats (25).

p47phox$^{-/-}$ aortas have decreased ROS production. Based on our in vitro observations that p47*phox* was necessary for NADPH oxidase activity and growth in SMCs, we hypothesized that the same phenomena could be examined in vivo in frozen sections from mouse aortas. We first demonstrated that frozen sections of aortas could reduce nitroblue tetrazolium in an NADH-dependent fashion that was inhibitable by diphenyliodonium (see Supplemental Data 3, www.jci.org/cgi/content/full/108/10/1513/DC3), which indicates that the NADH oxidase is still functional in freshly frozen sections. The capacity for ROS generation was measured in situ in wild-type and p47*phox*$^{-/-}$ aortas using a previously validated assay (37, 38) (Figure 5). Fresh-frozen cross sections of aorta were incubated with DHE, the conversion of which to ethidium served as a marker for O_2^-. Wild-type aortas (left panels) had consistently increased DHE fluorescence compared with p47*phox*$^{-/-}$ aortas (right panels), indicating that aortas from p47*phox*$^{-/-}$ mice had lower basal production of O_2^- than did aortas from wild-type mice. (DHE fluorescence under these conditions was inhibitable by treatment with superoxide dismutase, demonstrating the specificity of fluorescence.) Quantitative analysis demonstrates that DHE fluorescence was decreased by 80% in p47*phox*$^{-/-}$ aortas.

ApoE$^{-/-}$/p47phox$^{-/-}$ aortas have decreased lesion size compared with ApoE$^{-/-}$ aortas. Our in vitro data, describing the contributions of NADPH oxidase and intracellular ROS to SMC proliferation, and the essential role that SMC growth and migration are felt to contribute to atherosclerotic lesion formation (39), provide a compelling argument to compare atherosclerotic lesion formation in ApoE$^{-/-}$/p47*phox*$^{-/-}$ mice and ApoE$^{-/-}$ mice. Mice were either maintained on a chow diet for 30 weeks or fed a high-fat "Western" diet for 10 weeks. Although ApoE$^{-/-}$ mice do develop atherosclerotic lesions (albeit more slowly) on a normal diet, we felt that studies using the high-fat diet were necessary in case p47*phox* deficiency resulted in a dramatic decrease in ROS production and lesion formation. To assess whether our findings resulted from differences in serum lipid levels, serum cholesterol and triglyceride levels were determined in wild-type, p47*phox*$^{-/-}$, ApoE$^{-/-}$, and ApoE$^{-/-}$/p47*phox*$^{-/-}$ mice. There was no effect of p47*phox* deficiency on serum lipid profiles in mice maintained on chow or high-fat diets (Table 1).

Lesion size was determined by two methods. Aortic sinus lesion area was determined by serial sectioning of the sinus followed by oil red O staining and analysis of intimal area. This method was chosen because it was the method used by previous investigators to evaluate the effect of NADPH oxidase deficiency on lesion size (27, 28). Because aortic sinus atherosclerosis progresses very rapidly in ApoE$^{-/-}$ mice, we also examined atherosclerotic lesions in the aorta, where the progression is more similar to that observed in human atherosclerosis. Whole aortic lesion area was determined in these animals by isolation of the aorta from the arch to the

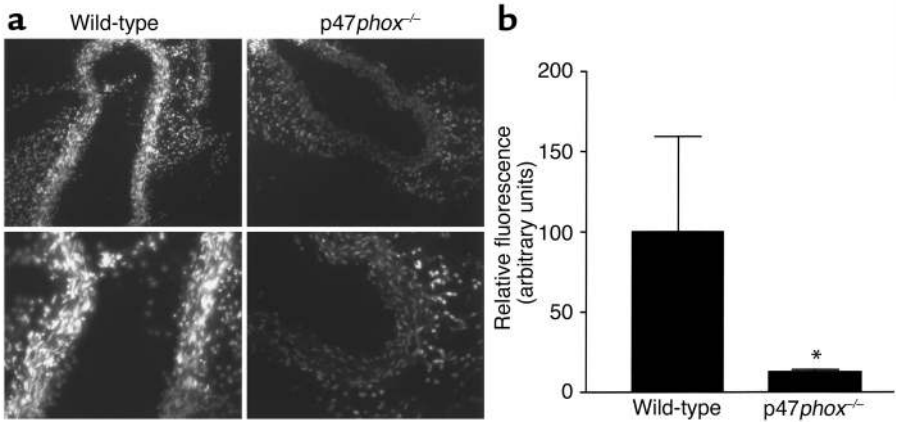

Figure 5
DHE staining is decreased in p47*phox*-deficient aortas compared with wild-type. (**a**) Fresh-frozen wild-type (left panels) and p47*phox*-deficient (right panels) aortas were stained for 10 minutes with DHE. Results are typical of staining of sections from four different aortas. (**b**) Digital scans of intimal regions of DHE-stained aortas from wild-type and p47*phox*-deficient mice were quantified using NIH Image software. Results shown are mean ± SD. *$P < 0.05$ compared with wild-type aortas.

Table 1
Blood lipid levels

Serum cholesterol levels (mg/dl ± SD)		
Genotype	Diet	
	Chow	High fat
Wild-type	52.1 ±14.7	198.2 ± 22.4
p47*phox*$^{-/-}$	48.6 ± 21.9	175.3 ± 30.7
ApoE$^{-/-}$	245 .2 ± 25.6	435.5 ± 26.9
ApoE$^{-/-}$/p47*phox*$^{-/-}$	229.7 ± 33.2	395.1 ± 54.3
Serum triglyceride levels (mg/dl ± SD)		
Genotype	Diet	
	Chow	High fat
Wild-type	53.4 ± 12.5	93.6 ± 19.2
p47*phox*$^{-/-}$	49.5 ± 9.9	83.4 ± 11.8
ApoE$^{-/-}$	78.7 ± 19.8	157.8 ± 24.5
ApoE$^{-/-}$/p47*phox*$^{-/-}$	68.9 ± 7.3	134.5 ± 40.9

bifurcation, staining of lesions with oil red O, and analysis of lesion area on whole mounts of the tissue. Comparisons were made among wild-type, p47*phox*$^{-/-}$, ApoE$^{-/-}$, and ApoE$^{-/-}$/p47*phox*$^{-/-}$ mice fed either a normal chow diet or a high-fat diet.

ApoE$^{-/-}$ and ApoE$^{-/-}$/p47*phox*$^{-/-}$ mice maintained on the chow diet (Figure 6) exhibited significant differences in total aortic lesion area (**$P < 0.005$). Lack of the p47*phox* protein in ApoE$^{-/-}$ mice was associated with a total mean lesion area that was 75% less than the mean lesion area in ApoE$^{-/-}$ mice (Figure 6a; representative aortas shown in Figure 6c). ApoE$^{-/-}$/p47*phox*$^{-/-}$ mice maintained on a high-fat diet for 10 weeks also had a significantly lower mean lesion area than ApoE$^{-/-}$ mice on a similar diet (Figure 7a, **$P < 0.05$). Of interest, and consistent with the findings of others (27, 28), there were no differences in mean aortic sinus lesion area between ApoE$^{-/-}$ and ApoE$^{-/-}$/p47*phox*$^{-/-}$ mice on either the chow or the high-fat diet (Figures 6b and 7b).

Recruitment of macrophages to atherosclerotic lesions does not require macrophage p47phox. To test whether macrophage recruitment was altered by disruption of the macrophage NADPH oxidase, macrophages were recruited from wild-type or p47*phox*$^{-/-}$ mice, and their ability to home to atherosclerotic lesions in ApoE$^{-/-}$ mice was measured at the luminal surface, in plaques (below the luminal surface), or in total (the sum of the number in plaques or at the luminal surface). The number of macrophages homing to lesions per mouse was compared between wild-type and p47*phox*$^{-/-}$ macrophages (Figure 8). The results are shown as the mean number attached ± SD ($n = 10$). No differences were observed in the ability of macrophages from wild-type or p47*phox*$^{-/-}$ mice to home to lesions, indicating that differences in macrophage homing per se do not account for the phenotypes of p47*phox*$^{-/-}$/ApoE$^{-/-}$ mice.

Discussion

It has been hypothesized that oxidative stress is a major element in the pathophysiology of vascular diseases; however, direct evidence of this hypothesis is lacking. Several enzyme systems, including the lipoxygenase, xanthine oxidase, and NADPH oxidase systems have been postulated to contribute to ROS generation in vascular cells (40, 41), but the relative contributions of each of these oxidase systems is unknown. There are several pathways by which O_2^- generated by arterial cells could promote atherosclerosis. We previously established that generation of both H_2O_2 and O_2^- occurs rapidly in human SMCs after thrombin stimulation, and that production of ROS is concomitant with increased NADH consumption and increased expression of p47*phox*.

Numerous investigators have demonstrated that ROS have direct mitogenic effects on vascular cells and are necessary intermediates for SMC mitogens such as

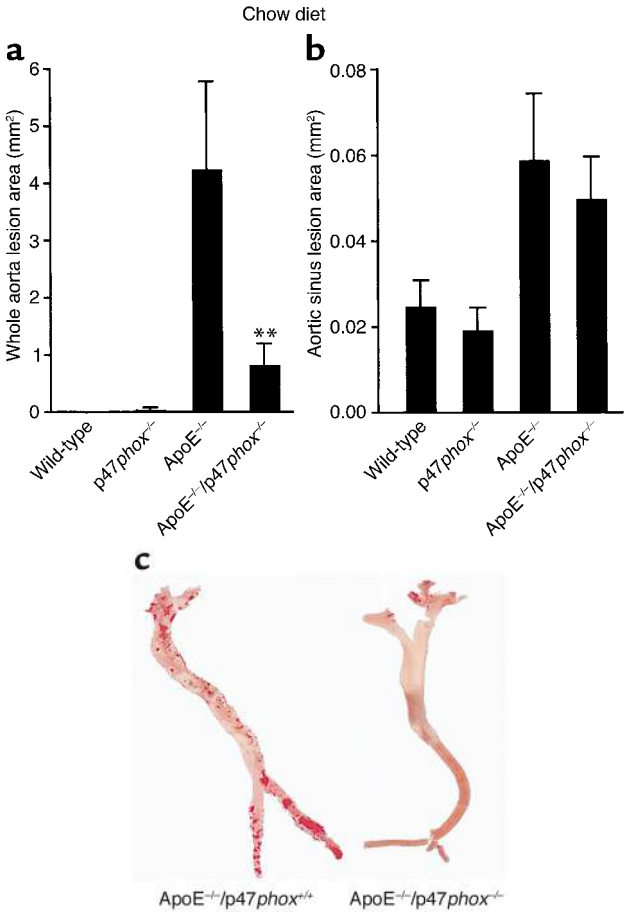

Figure 6
Comparison of oil red O–positive lesion size in mice on chow diet. Lesions were measured in whole aortas (**a**) and the aortic sinus (**b**). Aortas taken from 30-week-old ApoE$^{-/-}$/p47*phox*$^{-/-}$ male mice maintained on a normal chow diet had decreased total aortic lesion size compared with ApoE$^{-/-}$ mice of the same age. There is a decrease of approximately 75% in lesion size in ApoE$^{-/-}$/p47*phox*$^{-/-}$ mice compared with ApoE$^{-/-}$ mice at this age. There is no detectable difference in atherosclerotic lesion size between these two genotypes when the aortic sinus lesions are compared (**b**). Representative oil red O–stained aortic specimens are shown in (**c**). **$P < 0.005$.

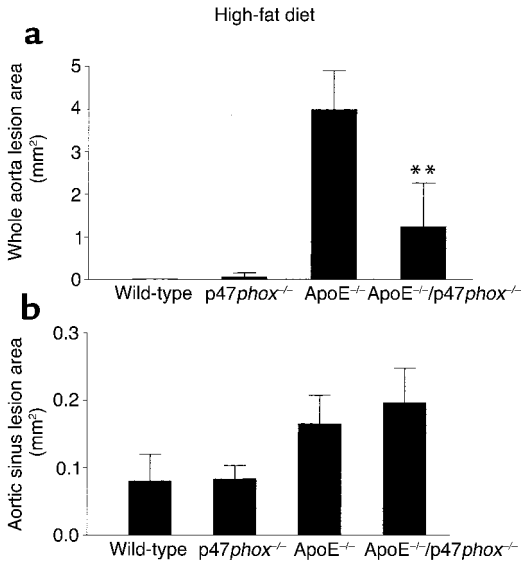

Figure 7
Comparison of oil red O–positive lesion size in mice on a high-fat diet. Lesions were measured from whole aortas (**a**) and the aortic sinus (**b**). Aortas from 18-week-old ApoE$^{-/-}$/p47*phox*$^{-/-}$ male mice maintained on a high-fat diet for 10 weeks had decreased total aortic lesion size compared with ApoE$^{-/-}$ mice of the same age. There is an approximately 67% decrease in lesion size in ApoE$^{-/-}$/p47*phox*$^{-/-}$ mice compared with ApoE$^{-/-}$ mice on a high-fat diet. There is no detectable difference between these two genotypes when the aortic sinus lesions are compared (**b**). $^{**}P < 0.05$.

PDGF and thrombin (25, 42, 43). The mechanism (or mechanisms) by which ROS stimulate SMC proliferation is not clear but may include increased calcium ion levels, changes in redox state of intracellular proteins, and/or activation of signaling pathways. Several investigators have demonstrated that NADPH oxidase is a necessary component for SMC responses to PDGF and angiotensin II stimulation (4, 19, 26, 28). In addition to promoting SMC hypertrophy, O_2^- production by vascular cells could result in oxidation of LDL, and oxidized LDL is a known atherogenic factor. O_2^- can also combine with nitric oxide to form peroxynitrite, a potent oxidizing species, which can also oxidize LDL.

We report here that expression of a component of NADPH oxidase, p47*phox*, is necessary for SMC response to growth factors and atherosclerotic lesion formation. Since there is no specific inhibitor for NADPH oxidase, the role of the enzyme can only be implicated indirectly from studies utilizing inhibitors. To overcome this obstacle, and to definitively determine whether the p47*phox* subunit of NADPH oxidase is necessary for SMC response to growth factors, we isolated aortic SMCs from wild-type and p47*phox*-deficient mice and compared their responses to growth factors. We found that p47*phox*-deficient cells have a decreased response to both thrombin and serum, clearly indicating that the oxidase is necessary for normal growth factor response. Basal and stimulated levels of ROS production in p47*phox*-deficient cells are also significantly decreased compared with wild-type cells. As a point of comparison for these studies, we also examined SMCs from gp91*phox*$^{-/-}$ mice, since gp91 is not required by the SMC NADPH oxidase. SMCs from gp91*phox*$^{-/-}$ mice responded to growth factors and produced ROS at the same level as did SMCs from wild-type mice. It is likely that in SMCs, *mox1* substitutes for gp91*phox* in NADPH oxidase (22, 23, 44).

Not only is p47*phox* an essential component of the SMC NADPH oxidase, its expression is upregulated by serum and thrombin in vitro. Interestingly, p47*phox* expression is also upregulated by the atherosclerotic process in vivo. As in our prior study in which we found increased p47*phox* protein present in balloon-injured rat aorta (25), we also found increased p47*phox* protein in atherosclerotic mouse aorta. These findings implicate NADPH oxidase in settings in which there is increased SMC growth.

We determined that p47*phox* (and NADPH oxidase activity) was important for atherosclerotic lesion development by comparing total aortic lesion area in atherogenic mice versus atherogenic mice deficient in p47*phox*. It should be noted that two similar studies using p47*phox*$^{-/-}$ and gp91*phox*$^{-/-}$ animals to determine whether NADPH oxidase is important in vascular lesion formation in ApoE$^{-/-}$ mice have been reported (27, 28). In both cases, investigators determined lesion formation by serial sectioning of the proximal aorta, predominantly in the area of the aortic sinus. In both cases, there was no difference observed in atherosclerotic lesion formation between ApoE$^{-/-}$ mice and either ApoE$^{-/-}$/p47*phox*$^{-/-}$ or ApoE$^{-/-}$/ gp91*phox*$^{-/-}$ mice. The major difference in our study was that we examined lesion formation along the entire length of the aorta, which allowed us to examine lesion formation at a much less advanced stage. For example, under the conditions used in our study, essentially the

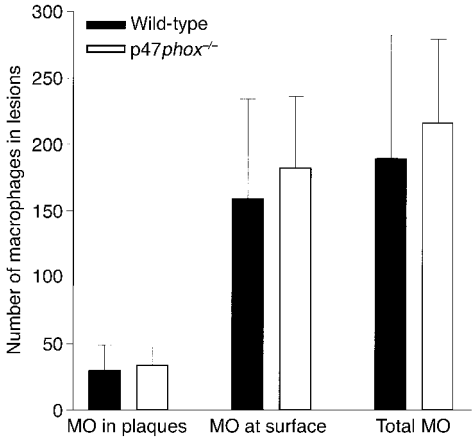

Figure 8
Comparison of ability of wild-type and p47*phox*$^{-/-}$ macrophages (MO) to home to atherosclerotic lesions in plaques, at the luminal surface, or in total, in ApoE$^{-/-}$ mice. No differences were observed in homing of macrophages of either genotype to lesions in ApoE$^{-/-}$ mice.

entire aortic sinus develops atherosclerosis in ApoE$^{-/-}$ mice, while less than 50% of the aortic surface contains oil red O–positive lesions.

By quantitating lesions throughout the aorta, we found that animals deficient in the p47*phox* protein in the ApoE$^{-/-}$ background had decreased total lesion formation compared with ApoE$^{-/-}$ animals, regardless of diet (chow diet or Western, high-fat diet). However, no difference in atherosclerotic lesion size was observed at the aortic sinus. There are at least two possible explanations for our results: (a) if the degree of lesion formation is quite advanced and covers the entire area examined, it is probably too late a stage to determine differences in lesion formation, and (b) it is possible that there are differences between lesion formation at the aortic sinus and elsewhere in ApoE$^{-/-}$ mice that are not well understood.

Deletion of the p47*phox* subunit was not cell- or tissue-specific in these animals; therefore all cell types involved in lesion formation were affected. This included a major cellular component of atherosclerotic lesions: macrophages and their progeny, foam cells. It is well known that O_2^- generation by phagocytic cells is crucial to host defense but may also be involved in the pathogenesis of atherosclerosis (2, 45, 46), and the major source of ROS production in phagocytic cells is NADPH oxidase. In an attempt to assess this, we also measured the ability of macrophages deficient in p47*phox* to home to atherosclerotic lesions, in comparison with wild-type macrophages. Interestingly, p47*phox*-deficient macrophages homed to lesions as efficiently as wild-type macrophages did, indicating that alterations of this component of the macrophage response does not account for differences in lesion formation in p47*phox*-deficient mice. Although our studies provide convincing evidence for involvement of the vascular NADPH oxidase in atherosclerosis, and demonstrate specific phenotypic defects in p47*phox*$^{-/-}$ SMCs, further studies will be required to determine the contributions of the oxidase in other cell types to the overall vascular response.

In summary, the studies reported here indicate that NADPH oxidase is necessary for normal atherogenic lesion progression in ApoE$^{-/-}$ mice. Although epidemiologic studies in humans and in vitro experimental studies have provided a rationale for examining the role of ROS generation in atherosclerosis, until now there has been little data from in vivo studies to support the general hypothesis that ROS in general, and specifically NADPH oxidase, is required for the atherogenic phenotype. Although deficiency of essential components of the oxidase does not eliminate lesion formation, it significantly reduces total lesion size throughout the length of the aorta. We have also established the necessity of NADPH oxidase in serum- and thrombin-induced SMC proliferation. SMC hypertrophy is a well-established component of atherogenic lesion formation, and NADPH oxidase can be activated by many factors that have roles in the formation of vascular lesions in vivo, including PDGF, angiotensin II, arachidonic acid, and phosphatidic acid. Long-term production of ROS by NADPH oxidase in SMCs and other vascular cells could result in sustained mitogenic effects of growth factors and significant pathophysiology, and ultimately in accelerated atherosclerotic lesion formation.

Acknowledgments

This work was supported by grants from NIH (HL-57352 and HL-59652, both to M.S. Runge).

1. Halliwell, B. 1989. Free radicals, reactive oxygen species and human disease: a critical evaluation with special reference to atherosclerosis. *Br. J. Exp. Pathol.* **70**:737–757.
2. Ohara, Y., Peterson, T.E., and Harrison, D.G. 1993. Hypercholesterolemia increases endothelial superoxide anion production. *J. Clin. Invest.* **91**:2546–2557.
3. Schleicher, E.D., Wagner, E., and Nerlich, A.G. 1997. Increased accumulation of the glycoxidation product N(epsilon)-(carboxymethyl)lysine in human tissues in diabetes and aging. *J. Clin. Invest.* **99**:457–468.
4. Rajagopalan, S., et al. 1996. Angiotensin II-mediated hypertension in the rat increases vascular superoxide production via membrane NADH/NADPH oxidase activation. *J. Clin. Invest.* **97**:1916–1923.
5. Steinberg, D. 1995. Role of oxidized LDL and antioxidants in atherosclerosis. *Adv. Exp. Med. Biol.* **369**:39–48.
6. Daugherty, A., and Roselaar, S.E. 1995. Lipoprotein oxidation is a mediator of atherogenesis: insights from pharmacological studies. *Cardiovasc. Res.* **29**:297–311.
7. Jones, S.A., Hancock, J.T., Jones, O.T.G., Newbauer, A., and Topley, N. 1995. The expression of NADPH oxidase components in human glomerular mesangial cells: detection of protein and mRNA for p47phox, p67phox, and p22phox. *J. Am. Soc. Nephrol.* **5**:1483–1491.
8. Jones, S.A., Wood, J.D., Coffey, M.J., and Jones, O.T.G. 1994. The functional expression of p47-phox and p67-phox may contribute to the generation of superoxide by an NADPH oxidase-like system in human fibroblasts. *FEBS Lett.* **335**:178–182.
9. Meier, B.M., Cross, A.R., Hancock, J.T., Kaup, F.J., and Jones, O.T.G. 1991. Identification of a superoxide-generating NADPH oxidase system in human fibroblasts. *Biochem. J.* **275**:241–245.
10. Neale, T.J., et al. 1993. Reactive oxygen species and neutrophil respiratory burst cytochrome b558 are produced by kidney glomerular cells in passive Heymann nephritis. *Proc. Natl. Acad. Sci. USA.* **90**:3645–3649.
11. Steinbeck, M.J., Appel, W.H., Verhoeven, A.J., and Karnovsky, M.J. 1994. NADPH-oxidase expression and in situ production of superoxide by osteoclasts actively resorbing bone. *J. Cell Biol.* **126**:765–772.
12. Segal, A.W., and Abo, A. 1993. The biochemical basis of the NADPH oxidase of phagocytes. *Trends Biochem. Sci.* **18**:43–47.
13. Griendling, K.K., Minieri, C.A., Ollerenshaw, J.D., and Alexander, R.W. 1994. Angiotensin II stimulates NADH and NADPH oxidase activity in cultured vascular smooth muscle cells. *Circ. Res.* **74**:1141–1148.
14. Matsubara, T., and Ziff, M. 1986. Superoxide anion release by human endothelial cells: synergism between a phorbol ester and a calcium ionophore. *J. Cell Physiol.* **127**:207–210.
15. Meier, B.M., Jesaitis, A.J., Emmendorffer, A., Roesler, J., and Quinn, M.T. 1993. The cytochrome b-558 molecules involved in the fibroblast and polymorphonuclear leucocyte superoxide-generating NADPH oxidase systems are structurally and genetically distinct. *Biochem. J.* **289**:481–486.
16. Inanami, O., et al. 1998. Activation of the leukocyte NADPH oxidase by phorbol ester requires the phosphorylation of p47PHOX on serine 303 or 304. *J. Biol. Chem.* **273**:9539–9543.
17. Bayraktutan, U., Draper, N., Lang, D., and Shah, A.M. 1998. Expression of functional neutrophil-type NADPH oxidase in cultured rat coronary microvascular endothelial cells. *Cardiovasc. Res.* **38**:256–262.
18. Jones, S.A., et al. 1996. Expression of phagocyte NADPH oxidase components in human endothelial cells. *Am. J. Physiol.* **271**:H1626–H1634.
19. Ushio-Fukai, M., Zafari, A.M., Fukui, T., Ishizaka, N., and Griendling, K.K. 1996. p22phox is a critical component of the superoxide-generating NADH/NADPH oxidase system and regulates angiotensin II-induced hypertrophy in vascular smooth muscle cells. *J. Biol. Chem.* **271**:23317–23321.
20. DeKeulaner, G.W., Alexander, R.W., Ushio-Fukai, M., Ishizaka, N., and Griendling, K.K. 1998. Tumour necrosis factor alpha activates a p22phox-based NADH oxidase in vascular smooth muscle. *Biochem. J.* **329**:653–657.
21. Wang, H.D., et al. 1998. Superoxide anion from the adventitia of the rat thoracic aorta inactivates nitric oxide. *Circ. Res.* **82**:810–818.

22. Fukui, T., Lasseque, B., Kai, H., Alexander, W.R., and Griendling, K.K. 1995. Cytochrome b-558 alpha-subunit cloning and expression in rat aortic smooth muscle cells. *Biochim. Biophys. Acta.* **1231**:215–219.
23. Suh, Y.A., et al. 1999. Cell transformation by the superoxide-generating oxidase Mox1. *Nature.* **401**:79–82.
24. Griendling, K.K., and Ushio-Fukai, M. 1998. Redox control of vascular smooth muscle proliferation. *J. Lab. Clin. Med.* **132**:9–15.
25. Patterson, C., et al. 1999. Stimulation of a vascular smooth muscle cell NAD(P)H oxidase by thrombin: evidence that p47(phox) may participate in forming this oxidase in vitro and in vivo. *J. Biol. Chem.* **274**:19814–19822.
26. Marumo, T., Schini-Kerth, V.B., Fisslthaler, B., and Busse, R. 1997. Platelet-derived growth factor-stimulated superoxide anion production modulates activation of transcription factor NF-kappaB and expression of monocyte chemoattractant protein 1 in human aortic smooth muscle cells. *Circulation.* **96**:2361–2367.
27. Hsich, E., et al. 2000. Vascular effects following homozygous disruption of p47(phox): an essential component of NADPH oxidase. *Circulation.* **101**:1234–1236.
28. Kirk, E.A., et al. 2000. Impaired superoxide production due to a deficiency in phagocyte NADPH oxidase fails to inhibit atherosclerosis in mice. *Arterioscler. Thromb. Vasc. Biol.* **20**:1529–1535.
29. Blank, R.S., Thompson, M.M., and Owens, G.K. 1988. Cell cycle versus density dependence of smooth muscle alpha actin expression in cultured rat aortic smooth muscle cells. *J. Cell Biol.* **107**:299–306.
30. Patterson, C., et al. 1996. Downregulation of vascular endothelial growth factor receptors by tumor necrosis factor-alpha in cultured human vascular endothelial cells. *J. Clin. Invest.* **98**:490–496.
31. Ruef, J., et al. 1997. Induction of vascular endothelial growth factor in balloon-injured baboon arteries: a novel role for reactive oxygen species in atherosclerosis. *Circ. Res.* **81**:24–33.
32. Kuppuswamy, D., et al. 1997. Association of tyrosine-phosphorylated c-Src with the cytoskeleton of hypertrophying myocardium. *J. Biol. Chem.* **272**:4500–4508.
33. Lomax, K.J., Leto, T.L., Nunoi, H., Gallin, J.I., and Malech, H.L. 1989. Recombinant 47-kilodalton cytosol factor restores NADPH oxidase in chronic granulomatous disease. *Science.* **245**:409–412.
34. Gardner, P.R., Nguyen, D.D.H., and White, C.W. 1994. Aconitase is a sensitive and critical target of oxygen poisoning in cultured mammalian cells and in rat lungs. *Proc. Natl. Acad. Sci. USA.* **91**:12248–12252.
35. Paigen, B., Morrow, A., Homes, P.A., Mitchell, D., and Williams, R.A. 1987. Quantitative assessment of atherosclerotic lesions in mice. *Atherosclerosis.* **68**:231–240.
36. George, J., et al. 1999. Enhanced fatty streak formation in C57BL/6J mice by immunization with heat shock protein-65. *Arterioscler. Thromb. Vasc. Biol.* **19**:505–510.
37. Pritchard, K.A., Jr., et al. 2001. Heat shock protein 90 mediates the balance of nitric oxide and superoxide anion from endothelial nitric-oxide synthase. *J. Biol. Chem.* **276**:17621–17624.
38. Miller, F.J., Jr., Gutterman, D.D., Rios, D., Heistad, D.D., and Davidson, B.L. 1998. Superoxide production in vascular smooth muscle contributes to oxidative stress and impaired relaxation in atherosclerosis. *Circ. Res.* **82**:1298–1305.
39. Andres, V. 1998. Control of vascular smooth muscle cell growth and its implication in atherosclerosis and restenosis. *Int. J. Mol. Med.* **2**:81–89.
40. Hedrick, C.C., Kim, M.D., Natarajan, R.D., and Nadler, J.L. 1999. 12-Lipoxygenase products increase monocyte:endothelial interactions. *Adv. Exp. Med. Biol.* **469**:455–460.
41. Berk, B.C. 1999. Redox signals that regulate the vascular response to injury. *Thromb. Haemost.* **82**:810–817.
42. Callsen, D., Sandau, K.B., and Brune, B. 1999. Nitric oxide and superoxide inhibit platelet-derived growth factor receptor phosphotyrosine phosphatases. *Free Radic. Biol. Med.* **26**:1544–1553.
43. Brar, S.S., et al. 1999. Requirement for reactive oxygen species in serum-induced and platelet-derived growth factor-induced growth of airway smooth muscle. *J. Biol. Chem.* **274**:20017–20026.
44. Pagano, P.J. 2000. Vascular gp91(phox): beyond the endothelium. *Circ. Res.* **87**:1–3.
45. Heinecke, J.W. 1998. Oxidants and antioxidants in the pathogenesis of atherosclerosis: implications for the oxidized low density lipoprotein hypothesis. *Atherosclerosis.* **141**:1–15.
46. White, C.R., et al. 1994. Superoxide and peroxynitrite in atherosclerosis. *Proc. Natl. Acad. Sci. USA.* **91**:1044–1048.